J Physiol 587.18 (2009) pp 4393–4404

The Journal of Physiology

Regulation of apoptotic potassium currents by coordinated zinc-dependent signalling

Patrick T. Redman[1], Karen A. Hartnett[1], Mandar A. Aras[1], Edwin S. Levitan[2] and Elias Aizenman[1]

Departments of [1]Neurobiology and [2]Pharmacology and Chemical Biology, University of Pittsburgh School of Medicine, Pittsburgh, PA 15261, USA

Oxidant-liberated intracellular Zn^{2+} regulates neuronal apoptosis via an exocytotic membrane insertion of Kv2.1-encoded ion channels, resulting in an enhancement of voltage-gated K^+ currents and a loss of intracellular K^+ that is necessary for caspase-mediated proteolysis. In the present study we show that an N-terminal tyrosine of Kv2.1 (Y124), which is a known target of Src kinase, is critical for the apoptotic current surge. Moreover, we demonstrate that Y124 works in concert with a C-terminal serine (S800) target of p38 mitogen-activated protein kinase (MAPK) to regulate Kv2.1-mediated current enhancement. While Zn^{2+} was previously shown to activate p38, we show here that this metal inhibits cytoplasmic protein tyrosine phosphatase ε (Cyt-PTPε), which specifically targets Y124. Importantly, a point mutation of Y124 to a non-phosphorylatable residue or over-expression of Cyt-PTPε protects cells from injury. Kv2.1-encoded channels thus regulate neuronal survival by providing a converging input for two Zn^{2+}-dependent signal transduction cascades.

(Received 2 June 2009; accepted after revision 17 July 2009; first published online 21 July 2009)

Corresponding author E. Aizenman: Department of Neurobiology, University of Pittsburgh School of Medicine, E1456 BST, Pittsburgh, PA 15261, USA. Email: redox@pitt.edu

Abbreviations CHO, Chinese hamster ovary; Cyt-PTPε, cytoplasmic protein tyrosine phosphatase ε; DTDP, 2,2′-dithiodipyridine; MAPK, mitogen activated protein kinase; PP2, 4-amino-5-(4-chlorophenyl)-7-(*t*-butyl)pyrazolo[3,4-d]pyrimidine; PP3, 4-amino-7-phenylpyrazol[3,4-d]pyrimidine; SNARE, *N*-ethylmaleimide-sensitive factor attachment protein receptor; TPEN, *N,N,N′,N′*-tetrakis (2-pyridalmethyl) ethylenediamine.

K^+ efflux mediated by a surge of voltage-gated K^+ channel activity is a necessary component of neuronal apoptosis (Yu, 2003) upstream of caspase activation (McLaughlin *et al.* 2001). This current enhancement leads to reduced cytoplasmic K^+ concentrations, producing a permissive pro-apoptotic environment as the catalytic activity of both caspases and apoptotic nucleases increases at low ionic strength (Hughes & Cidlowski, 1999). This effect is significant because inhibiting K^+ efflux effectively attenuates apoptotic neuronal cell death (Yu *et al.* 1997; Aizenman *et al.* 2000*b*; McLaughlin *et al.* 2001; Bossy-Wetzel *et al.* 2004).

Kv2.1, a delayed rectifying potassium channel (Murakoshi & Trimmer, 1999; Malin & Nerbonne, 2002), is responsible for the apoptotic K^+ current surge in rat cortical neurons (Pal *et al.* 2003). Indeed, we previously showed that dominant negative constructs of Kv2.1 block the K^+ current enhancement in addition to providing neuroprotection against apoptotic insults (Pal *et al.* 2003). Furthermore, Kv2.1 expression in cells that express no endogenous voltage-gated K^+ channels, such as CHO cells (Yu & Kerchner, 1998), is sufficient for the induction of apoptosis following what would normally be a sub-lethal exposure to apoptogens (Pal *et al.* 2003). Following an oxidative insult, the liberation of intracellular Zn^{2+} from metal binding proteins (Aizenman *et al.* 2000*a*) facilitates the generation of signalling reactive oxygen species (Sensi & Jeng, 2004; Zhang *et al.* 2004) leading to the activation of p38 MAPK via the upstream apoptosis signalling kinase 1 (ASK-1) (McLaughlin *et al.* 2001; Aras & Aizenman, 2005). The subsequent enhancement of K^+ currents following Zn^{2+}-dependent p38 activation is mediated by the soluble *N*-ethylmaleimide-sensitive factor attachment protein receptor (SNARE)-dependent exocytotic plasma membrane insertion of new Kv2.1-encoded channels, rather than an alteration in the properties of existing membrane resident channels (Pal *et al.* 2003, 2006; Redman *et al.* 2007). Our group recently demonstrated that the Kv2.1-mediated current enhancement necessary to complete the apoptotic program in cortical neurons requires the direct phosphorylation of intracellular C-terminal residue serine 800 (S800) by p38 MAPK (Redman *et al.* 2007).

Kv2.1-mediated K^+ currents are also enhanced during non-injurious conditions through direct phosphorylation

DOI: 10.1113/jphysiol.2009.176321

of intracellular N-terminal residue tyrosine 124 (Y124) by Src kinase (Tiran *et al.* 2003, 2006). Since an elevation of cytoplasmic Zn^{2+}, a process directly linked to cell injury (Weiss *et al.* 2000), can also activate Src (Wu *et al.* 2002; Huang *et al.* 2008) in addition to p38 MAPK (McLaughlin *et al.* 2001), we sought to investigate the requirement of converging Src and p38 (Redman *et al.* 2007) signalling on the apoptotic Kv2.1 current surge and neuronal viability. We hypothesized that Zn^{2+}-dependent modulation of both intracellular termini may contribute to the apoptotic K^+ current surge, as an interaction between these domains is required for normal channel surface delivery (Mohapatra *et al.* 2008). In addition, exocytotic SNARE proteins physically associate with both N- and C-terminals (MacDonald *et al.* 2002; Leung *et al.* 2003; Tsuk *et al.* 2005; Lvov *et al.* 2008), and SNARE cleavage effectively abolishes channel surface delivery during apoptosis (Pal *et al.* 2006). Results presented here demonstrate that Y124 on Kv2.1 is a critical residue for the apoptotic surge of K^+ currents. In addition, both Y124 and S800 work in concert to influence cell viability via K^+ current enhancement in a Zn^{2+}-dependent fashion.

Methods

Plasmids and site-directed mutagenesis

Kv2.1 was the gift of J. Trimmer (UC Davis); Kv2.1(Y124F), Cyt-PTPε and Cyt-PTPε(D245A) were obtained from A. Elson (Weizmann Institute, Rehovot, Israel). Mutagenesis was performed using QuickChange XL (Stratagene, La Jolla, CA, USA) and confirmed by sequencing. Primers containing the desired mutations were from Integrated DNA Technologies (Coralville, IA, USA). Enhanced green fluorescent protein (pCMVIE-eGFP; Clontech, Palo Alto, CA, USA) was used for the visual identification of positively transfected cells. Of note, we found that the Y124D mutation of Kv2.1 did not mimic the phosphorylated state at this site (results not shown).

Tissue culture and transfection

Chinese hamster ovary (CHO) cells were plated at 5.6×10^4 cells per well on coverslips in 24-well plates 24 h prior to transfection. Cells were treated for 4 h in serum-free medium (F12 nutrient medium with 10 mM Hepes) with a total of 1.2 μl Lipofectamine (Invitrogen, Carlsbad, CA, USA) and 0.28 μg DNA per well. Following transfection, cells were maintained in F12 medium containing fetal bovine serum (FBS) for 24 h prior to recordings. Cortical neurons were prepared from embryonic day 16 rat embryos and grown in 6-well plates according to McLaughlin *et al.* (2001). To generate these cultures, one animal was generally killed per week by CO_2 inhalation in accordance with The University of Pittsburgh Institutional Animal Care and Use Committee and the policies and regulations outlined in 'Reporting ethical matters in *The Journal of Physiology*: standards and advice' (Drummond, 2009). Neurons (18–22 days *in vitro*) were transfected using Lipofectamine 2000 (Invitrogen; Ohki *et al.* 2001). Cells were then maintained at 37°C, 5% CO_2 for 24–48 h before drug treatment procedures and toxicity assays.

Drug treatments

The apoptotic stimulus for the electrophysiological experiments in CHO cells consisted of a 5 min treatment with 30 μM of the thiol oxidant apoptogen 2,2′-dithiodipyridine (DTDP) at 37°C, 5% CO_2. DTDP induces cell death by promoting the liberation of intracellular Zn^{2+} (Aizenman *et al.* 2000*b*). The DTDP-containing solution was then removed and replaced with fresh F12 medium containing 10 μM 1-3-boc-aspartyl (Ome)-fluoromethyl-ketone (BAF), a broad-spectrum cysteine protease inhibitor. BAF was necessary to maintain cells viable for electrophysiological recordings since Kv2.1-expressing cells are highly susceptible to DTDP-induced apoptosis (Pal *et al.* 2003). Electrophysiological recordings were performed approximately 3 h following oxidative injury, a time point where the current surge is well-established (McLaughlin *et al.* 2001). The apoptotic stimulus for the electrophysiological experiments in cortical neurons consisted of a 10 min treatment with either 30 or 60 μM DTDP at 37°C, 5% CO_2. The DTDP-containing solution was then removed and replaced with conditioned growth medium containing 10 μM BAF. For the Src inhibition experiments, either 10 μM 4-amino-5-(4-chlorophenyl)-7-(*t*-butyl)pyrazolo[3,4-d]pyrimidine (PP2) or 10 μM of the inactive structural analogue 4-amino-7-phenylpyrazol[3,4-d]pyrimidine (PP3) were included in the treatment solution and post-treatment medium.

Electrophysiological measurements

Current recordings were performed on GFP-positive CHO cells and cortical neurons using the whole-cell patch-clamp configuration technique (McLaughlin *et al.* 2001). Ninety seven per cent of GFP-positive CHO cells co-transfected with Kv2.1 had measurable K^+ currents (data not shown), while 90% of GFP-positive neurons are known to express co-transfected plasmids (Santos & Aizenman, 2002). The intracellular electrode solution contained (in mM): 100 potassium gluconate, 10 KCl, 1 $MgCl_2$, 1 $CaCl_2 \cdot 2H_2O$, 10 Hepes; pH adjusted to 7.2 with concentrated KOH; 0.22 mM ATP was added and the osmolarity was adjusted to 280 mosmol l^{-1} with sucrose.

The extracellular solution contained (in mM): 115 NaCl, 2.5 KCl, 2.0 $MgCl_2$, 10 Hepes, 0.1 BAPTA, 10 D-glucose, 0.1 tetrodotoxin; pH was adjusted to 7.2. Measurements were obtained under voltage-clamp conditions with an Axopatch 1-D amplifier (Axon Instruments, Foster City, CA, USA) and pCLAMP software (Axon instruments) using 2–3 MΩ electrodes. Series resistance was partially compensated (80%) in all cases. Currents were filtered at 2 kHz and digitized at 10 kHz. Potassium currents were evoked with incremental 10 mV voltage steps to +80 mV from a holding potential of −80 mV. Steady-state current amplitudes were measured at 180 ms after the initiation of the −80 mV to +10 mV step and normalized to cell capacitance. CHO cells ranged in capacitance from approximately 4 to 12 pF, while neurons had capacitance values ranging from approximately 8 to 30 pF. Differences in neuronal basal current densities may be attributable to changes in culture conditions over time. For example, the measurements shown in Figs 2 and 6 were obtained nearly a year apart. It is possible that cells that have elevated basal currents have adapted to some other condition within the culture, such as increased activity (Aizenman *et al.* 2003; Pratt & Aizenman, 2007). Regardless, all cells show a relative increase in amplitude following an apoptotic stimulus. All data are expressed as mean ± S.E.M. and statistical analyses were performed using InStat software (GraphPad, San Diego, CA, USA).

Neuronal zinc imaging

Wide-field Zn^{2+} fluorescent measurements were performed on neurons loaded with the Zn^{2+} indicator FluoZin-3 AM (30 min; 5 μM prepared in buffered solution containing 144 mM NaCl, 3 mM KCl, 10 mM Hepes, 5.5 mM glucose, 5 mg ml^{-1} bovine serum albumin; pH 7.3). The culture-containing glass coverslips were transferred to a recording chamber (Warner, Hamden, CT, USA) mounted on an inverted epifluorescence microscope superfused with phenol red-free MEM, supplemented with 25 mM Hepes and 0.01% BSA. Images were acquired by exciting the fluorescent dye with 490 nm light every 10 s for 10 min using a computer-controlled monochromator (Polychrome II, TILL photonics, Martinsried, Germany) and CCD camera (Imago, TILL photonics). Following acquisition of baseline metal levels (for approximately 100 s), neurons were exposed to DTDP (30 or 60 μM, 500 s). DTDP-induced Zn^{2+} fluorescence was then quenched by exposing cells to the membrane-permeant Zn^{2+} chelator *N,N,N′,N′*-tetrakis (2-pyridalmethyl) ethylenediamine (TPEN, 20 μM, 200 s). The magnitude of the Zn^{2+} signal for all neuronal cell bodies in a single field ($n = 10$–25 neurons) was determined by subtracting the fluorescence signal after TPEN perfusion from the maximal DTDP-induced signal (ΔF_{TPEN}). With this method, larger ΔF_{TPEN} values correspond to higher amounts of free intracellular Zn^{2+} liberated by DTDP (Knoch *et al.* 2008).

Cell-free phosphatase assay

FLAG-Cyt-PTPε transfected CHO cells were lysed in buffer A (50 mM Tris-HCl pH 7.5, 100 mM NaCl, 1% NP-40) (Tiran *et al.* 2006) containing protease inhibitors (Complete Mini protease inhibitor cocktail, Roche Applied Science, Indianapolis, IN, USA). FLAG-Cyt-PTPε-expressed protein was immunoprecipitated by incubating cell lysates with an anti-FLAG rabbit polyclonal antibody (Sigma-Aldrich Inc., St Louis, MO, USA) followed by protein A/G PLUS-agarose immunoprecipitation beads (Santa Cruz Biotechnology Inc., Santa Cruz, CA, USA). The immunoprecipitated complex was then washed 3 times with buffer A, 2 times in buffer B (100 mM KCl, 0.5 mM EDTA pH 8.2, 20 mM Hepes pH 7.6, 0.4% NP-40, 20% glycerol) and 2 times in buffer 54 K (150 NaCl, 50 mM Tris pH 7.9, 0.5% Triton X-100). FLAG-Cyt-PTPε was eluted by incubating the beads in two equal volumes of an elution buffer containing 50 mM MES pH 7, 0.5 mM DTT, 0.5 mg ml^{-1} BSA, and 1 mg ml^{-1} FLAG peptide. (Sigma-Aldrich Inc.) at 32°C for 3 min. Total protein was determined by a colourimetric protein assay (Bio-Rad, Hercules, CA, USA). Equal amounts of protein were added to the reaction mixtures. Phosphatase activity was then measured using a colourimetric malachite green-based assay (Promega Corp., Madison, WI, USA) using two chemically synthesized phospho-tyrosine peptides (Promega Corp.) END(pY)INASL (Daum *et al.* 1993) and DADE(pY)LIPQQG (Zhang *et al.* 1993) at 32°C for 18 h. The reaction was terminated by adding 50 μl of the molybdate–additive mixture, incubated at room temp for 15 min and then optical density of each sample was measured at 600 nm (1420 Victor^2 V Multilabel Counter, Perkin Elmer Life Sciences, Boston, MA, USA). Activity was expressed as picomoles phosphate released normalized to total Cyt-PTPε protein added to the reaction. A standard activity calibration curve was always performed with known amounts of free phosphate.

Viability assays

CHO cells were transfected with GFP and pRBG4 vector plus Kv2.1 or Kv2.1(Y124F). Twenty-four hours after transfection, cells were exposed to either 30 μM DTDP or vehicle for 15 min. Twenty-four hr following treatment, counts of GFP-positive cells were obtained from five random fields with a 20× objective per coverslip; three coverslips were counted per condition in three independent experiments. Cortical neurons were transfected after 3 weeks *in vitro* with equal amounts of pUHC13-3 Luciferase and either pCDNA3 vector or Cyt-PTPε plasmids (Boeckman

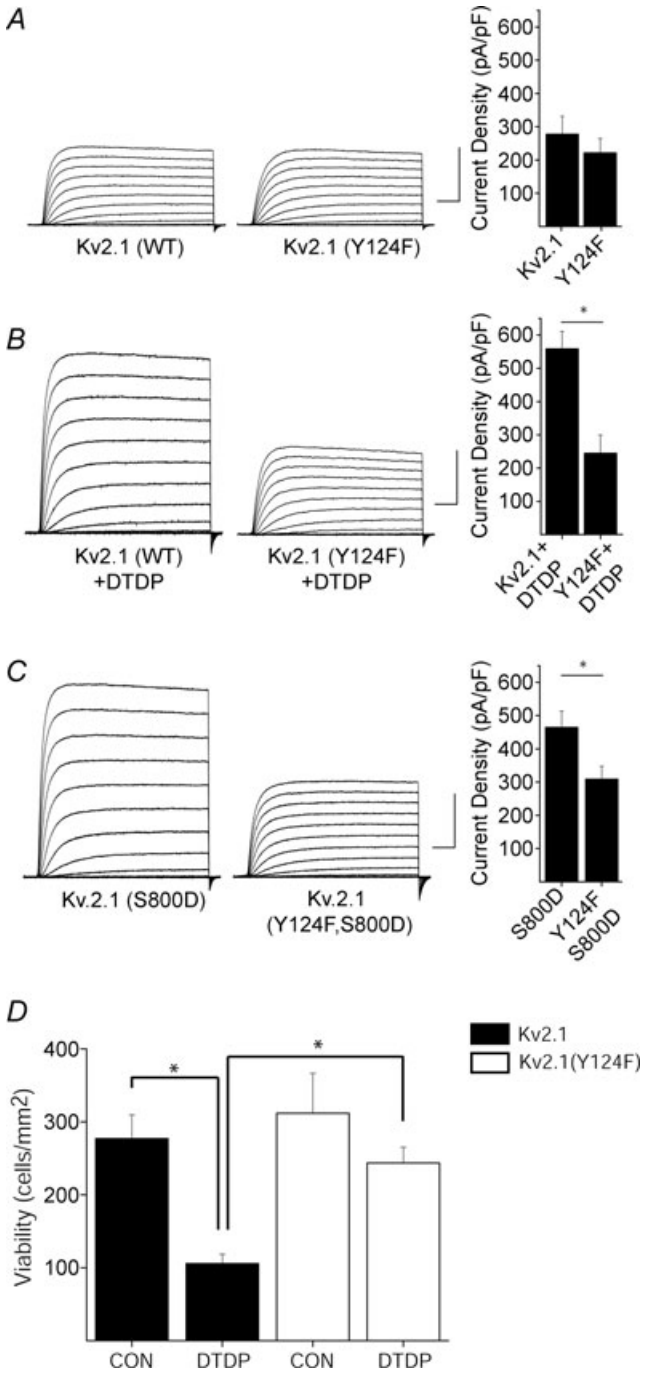

Figure 1. Y124 is essential for the apoptotic K^+ current surge
A (left), representative whole-cell K^+ currents from wild-type Kv2.1- and Kv2.1(Y124F)-expressing CHO cells. Currents were obtained 24 h post-transfection and evoked by sequential 10 mV voltage steps to +80 mV from a holding potential of −80 mV. Calibration: 5 nA, 25 ms. Right, mean ± S.E.M. current densities from wild-type Kv2.1-expressing ($n = 15$) and Kv2.1(Y124F)-expressing CHO cells ($n = 10$). *B* (left), representative whole-cell K^+ currents from wild-type Kv2.1- and Kv2.1(Y124F)-expressing CHO cells treated with DTDP. Calibration: 5 nA, 25 ms. Right, mean ± S.E.M. current densities from wild-type Kv2.1- ($n = 12$) and Kv2.1(Y124F)-expressing ($n = 9$) CHO cells (*$P < 0.05$; 2-tailed *t* test). *C* (left), representative currents from Kv2.1(S800D)- and Kv2.1(Y124F, S800D)-expressing CHO cells. Calibration: 5 nA, 25 ms. Right, mean ± S.E.M. current densities from Kv2.1(S800D)-expressing ($n = 11$) and Kv2.1(Y124F,S800D)-expressing ($n = 13$) CHO cells (*$P < 0.05$; 2-tailed *t* test). *D*, Y124F mutation disrupts Kv2.1-mediated apoptosis. CHO cells were cotransfected with eGFP plus empty vector and either Kv2.1 or Kv2.1(Y124F) and 24 h later exposed to 30 μM DTDP (15 min). Viability was assayed 24 h post-treatment by counting GFP-positive cells. Values represent the mean ± S.E.M. ($n = 3$) and are representative of 3 separate, independent experiments (*$P < 0.05$; ANOVA/Bonferroni).

& Aizenman, 1996; Pal *et al.* 2003). Untransfected rat microglial cells (Cheepsunthorn *et al.* 2001) were plated directly onto cortical neurons at a density of 50 000 cells per well 24 h following neuronal transfection. Microglia were then stimulated with 10 U ml^{-1} interferon-γ (IFN-γ, Chemicon, Temecula, CA, USA) and 1 μg ml^{-1} lipopolysaccharide (Knoch *et al.* 2008). Neuronal viability was measured 48 h later using a luminescence reporter assay (Perkin-Elmer) (Aras *et al.* 2008).

Results

Src kinase target Y124 in Kv2.1 is critical for the apoptotic surge of K^+ currents

CHO cells express no endogenous voltage-gated K^+ channels (Yu & Kerchner, 1998), and undergo apoptosis following Kv2.1 expression after a normally sub-lethal oxidative injury (Pal *et al.* 2003). As with neurons, Kv2.1-expressing CHO cells display enhanced voltage-gated K^+ currents during the cell death program (Pal *et al.* 2006). Recordings were obtained from CHO cells transiently expressing either wild-type Kv2.1 or phenylalanine-substituted, Kv2.1(Y124F) mutant channels. Phenylalanine substitution was used to preclude phosphorylation at this site. Under control conditions, cells expressing Kv2.1(Y124F) channels exhibited K^+ current densities similar to CHO cells expressing wild-type Kv2.1 channels (Fig. 1*A*). However, following exposure to DTDP, the characteristic K^+ current surge observed in wild-type Kv2.1-expressing cells was completely abrogated in cells expressing Kv2.1(Y124F) (Fig. 1*B*). The voltage-dependent activation profiles for both wild-type and mutant channels were nearly identical (online Supplemental Fig. 1), suggesting the single amino acid substitution did not alter gating kinetics. Indeed, the voltage for half-maximal activation remained unchanged for both channels (28.9 ± 2.75 mV for Kv2.1 ($n = 11$); 33.85 ± 2.82 mV for Kv2.1(Y124F) ($n = 8$).

We previously reported that phospho-mimicking serine-to-aspartate-substituted Kv2.1(S800D) mutant channels mimic the apoptotic K^+ current surge in CHO cells (Fig. 1*C*) (Redman *et al.* 2007). To further examine the requirement of Y124 in K^+ current

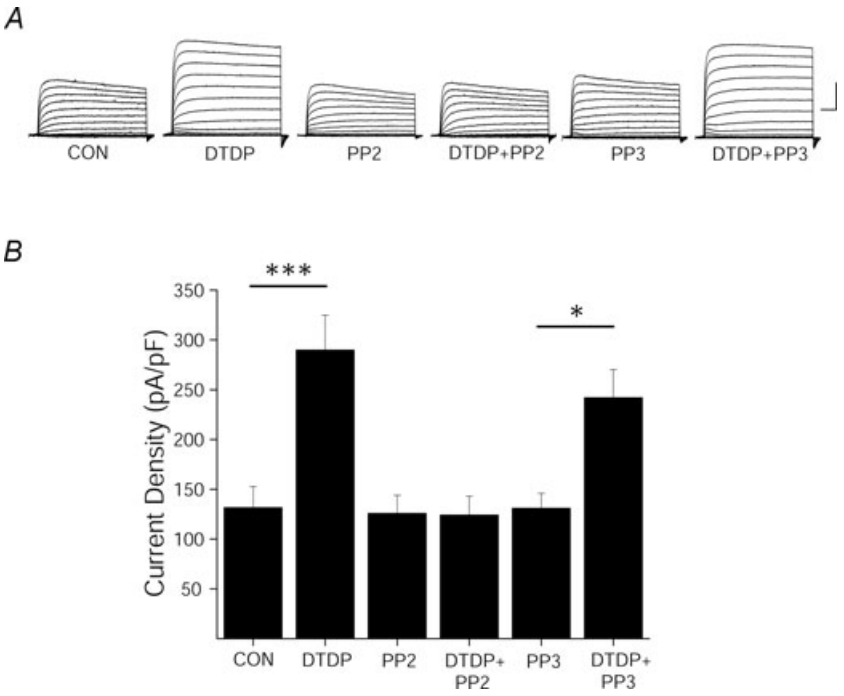

Figure 2. Src inhibition blocks the apoptotic K^+ current surge
A, representative whole-cell currents from cortical neurons recorded under control, DTDP (30 μM), PP2 (10 μM), DTDP + PP2, PP3 (10 μM), and DTDP + PP3 treatment conditions. Currents were obtained 3 h post-injury and evoked by sequential 10 mV voltage steps to +80 mV from a holding potential of −80 mV. Calibration: 5 nA, 25 ms *B*, mean ± S.E.M. current densities from cortical neurons recorded under control ($n = 13$), DTDP ($n = 14$), DTDP + PP2 ($n = 10$), PP2 ($n = 10$), PP3 ($n = 10$), and DTDP + PP3 ($n = 10$) treatment conditions. K^+ currents were evoked by a single voltage step to +10 mV from a holding potential of −80 mV and normalized to cell capacitance. (***$P < 0.001$, *$P < 0.05$; ANOVA/Bonferroni).

enhancement, we obtained recordings from CHO cells expressing Kv2.1(Y124F,S800D) double mutant channels. Here we observed that cells expressing double mutant Kv2.1(Y124F,S800D) channels displayed significantly reduced current densities compared to cells expressing Kv2.1(S800D) (Fig. 1*C*), suggesting that an intact Y124 is necessary for apoptotic Kv2.1-mediated current enhancement, and reinforcing the notion that both Y124 and S800 were critical for Kv2.1 modulation during the cell death process. In fact, since a mutation at Y124 was sufficient to block the enhancement of K^+ currents, we examined whether an intact tyrosine was also required to support apoptosis in Kv2.1-expressing CHO cells. DTDP treatment resulted in the death of approximately 50% of wild-type Kv2.1-expressing cells (Fig. 1*D*). This agent, however, produced substantially less toxicity in Kv2.1(Y124F)-expressing cells (Fig. 1*D*). Indeed, a significant, greater than 2-fold increase in viability was observed in Kv2.1(Y124F)-expressing cells when compared to wild-type Kv2.1-expressing cells. Because residue Y124 in Kv2.1 is a known target of Src (Tiran *et al.* 2003, 2006), we next examined whether inhibition of Src kinase itself limited K^+ current enhancement in two different experimental protocols. First, whole-cell recordings were obtained from cortical neurons, which natively express Kv2.1. As expected, neurons treated with DTDP displayed significantly enhanced K^+ currents compared to vehicle-treated controls (Fig. 2*A*, *B*). Recordings were also obtained following treatment of cortical neurons with DTDP and either the selective Src family kinase inhibitor PP2 (10 μM) or its inactive structural analogue PP3 (10 μM). We observed that the DTDP-induced apoptotic K^+ current enhancement in neurons was blocked by PP2 (10 μM), but not by negative control PP3 (10 μM; Fig. 2*A* and *B*). Notably, treatment of cortical neurons with either PP2 or PP3 alone had no effect on

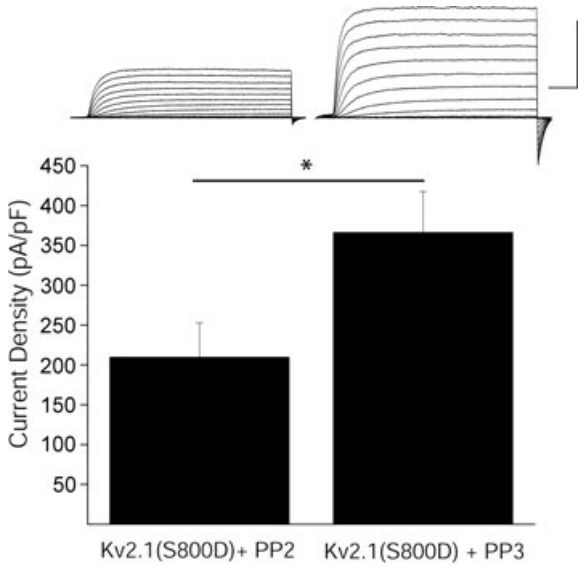

Figure 3. Src inhibition blocks elevated basal K^+ currents in Kv2.1(S800D)-expressing CHO cells
Top, representative whole-cell K^+ currents from Kv2.1(S800D)-expressing CHO cells recorded following treatment with either the Src family kinase inhibitor PP2 or the inactive structural analogue PP3. Calibration: 10 nA, 25 ms. Bottom, mean ± S.E.M. current densities from Kv2.1(S800D)-expressing CHO cells treated with PP2 ($n = 12$) or PP3 ($n = 10$) (*$P < 0.05$, 2-tailed *t* test).

baseline current densities (Fig. 2*A* and *B*). Next, we exposed CHO cells to either PP2 or PP3 immediately following transfection with the mutant construct Kv2.1(S800D) to further evaluate Src regulation of Kv2.1-mediated K^+ currents. Strikingly, whole-cell recordings performed 24 h following transfection revealed that PP2, but not PP3, limited the enhanced current densities expected for this phospho-mimicking mutant channel (Fig. 3). Taken together, these results establish the requirement for Src activity in the K^+ current surge in apoptotic neurons. Furthermore, these data suggest that a certain degree of basal Src kinase activity exists in CHO cells, which is necessary to observe the enhanced currents mediated by Kv2.1(S800D).

Role of Cyt-PTPε and Zn^{2+} on the apoptotic K^+ current surge

Cyt-PTPε dephosphorylates Y124, which can counteract enhanced Kv2.1 activity induced by

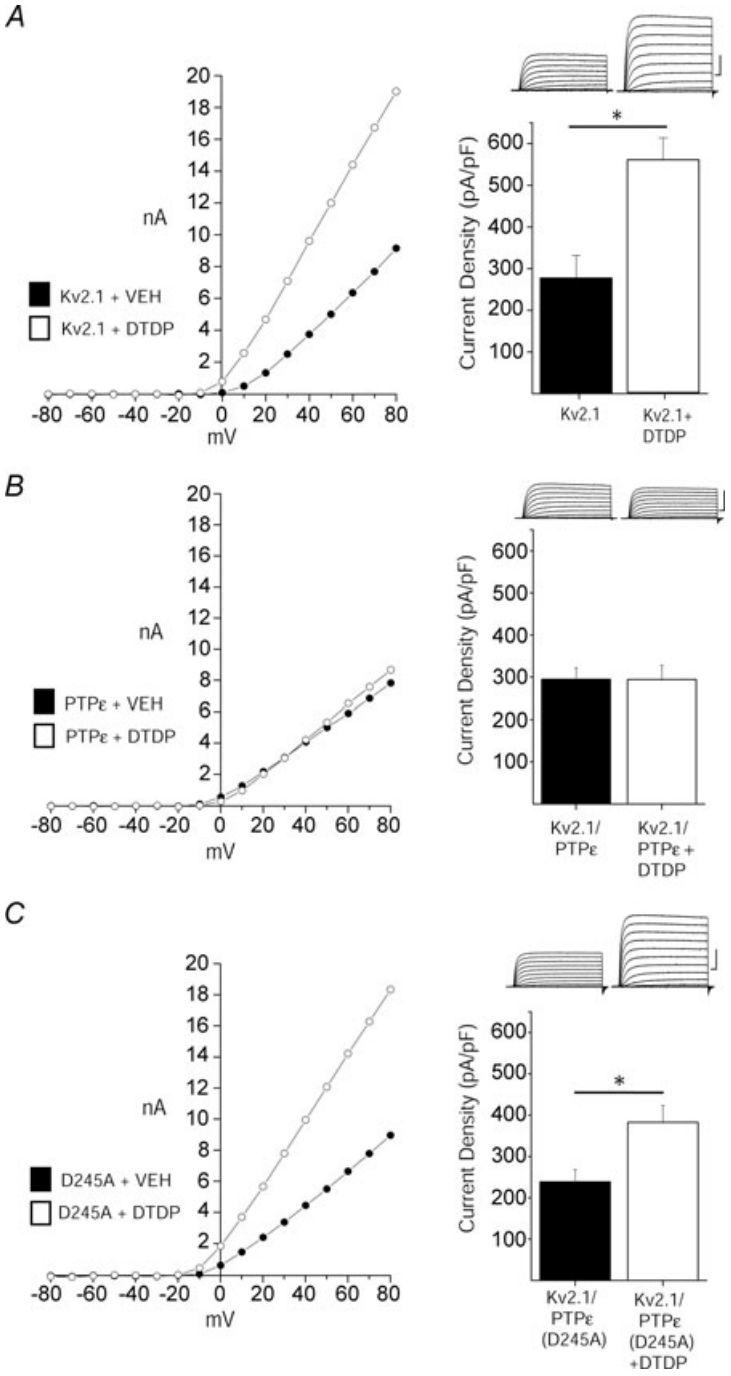

Figure 4. Cyt-PTPε blocks apoptotic K^+ current enhancement
A, DTDP induces current enhancement in Kv2.1-expressing CHO cells. Left, representative steady-state current–voltage relationship of Kv2.1-expressing CHO cells recorded following vehicle (filled) and DTDP treatment (open) conditions (30 μM for 5 min). Right, representative whole-cell currents and mean ± S.E.M. current densities from Kv2.1-expressing CHO cells recorded following vehicle ($n = 15$) and DTDP ($n = 12$) treatment conditions; bar graphs are the same as those shown in Fig. 1*A* and *B* for wild-type Kv2.1. *B*, Cyt-PTPε and Kv2.1 co-expression blocks apoptotic K^+ current densities in CHO cells. Left, representative steady-state current–voltage relationship of Kv2.1- and Cyt-PTPε-expressing CHO cells recorded following vehicle (filled) and DTDP treatment (open) conditions. Currents were obtained 3 h post-oxidative injury. Right, representative whole-cell currents and mean ± S.E.M. current densities from Kv2.1- and Cyt-PTPε-expressing CHO cells recorded under control ($n = 16$, filled) and DTDP treatment ($n = 16$, open) conditions. *C*, enzymatic activity of Cyt-PTPε is required for inhibition of apoptotic K^+ current enhancement. Left, representative steady-state current–voltage relationship of Kv2.1- and Cyt-PTPε(D245A)-expressing CHO cells recorded under control (filled) and DTDP treatment (open) conditions. Right, representative whole-cell currents and mean ± S.E.M. current densities from Kv2.1- and Cyt-PTPε(D245A)-expressing CHO cells recorded under control ($n = 16$, filled) and DTDP treatment ($n = 16$, open) conditions (*$P < 0.01$; 2-tailed *t* test). Current density was calculated as the steady-state K^+ current evoked by a single voltage step to +10 mV from a holding potential of −80 mV normalized to cell capacitance.

Src-mediated phosphorylation during non-injurious conditions (Tiran *et al.* 2003, 2006). Accordingly, we evaluated whether Cyt-PTPε over-expression would be sufficient to inhibit apoptotic K^+ current surges. Whole-cell recordings were performed in CHO cells co-expressing Kv2.1 and Cyt-PTPε following vehicle and DTDP treatment. We observed that Cyt-PTPε expression strongly inhibited the DTDP-induced K^+ current surge in Kv2.1-expressing cells (Fig. 4*A* and *B*), while co-expression of a catalytically inactive mutant isoform of this phosphatase (Cyt-PTPε-D245A) (Flint *et al.* 1997; Peretz *et al.* 2000) did not (Fig. 4*C*). Thus, enzymatic activity of this Kv2.1-targeting phosphatase is required for inhibition of the K^+ current surge. Moreover, Cyt-PTPε over-expression was also sufficient to prevent the elevated currents observed in Kv2.1(S800D)-expressing CHO cells (Fig. 5). Importantly, manipulation of Y124-targeting enzymes, first via Src inhibition and now by Cyt-PTPε over-expression, blocks the apoptotic K^+ current surge. These results show not only that Y124 is required, but it is likely to be phosphorylated to permit the apoptotic Kv2.1-mediated current enhancement.

Next, we performed recordings in vehicle- and DTDP-treated cortical neurons transfected with either empty vector or Cyt-PTPε to confirm that the phosphatase can influence the K^+ current surge in cells expressing Kv2.1-encoded channels endogenously. While vector-transfected neurons exhibited a robust, characteristic K^+ current surge following treatment with 30 μM DTDP (Fig. 6*A*), Cyt-PTPε-transfected neurons exhibited no K^+ current increase (Fig. 6*B*), similar to the previously noted observation in CHO cells. We noted, however, that higher concentrations of DTDP (i.e. 60 μM) were sufficient to overcome the effects of Cyt-PTPε over-expression (Fig. 6*A* and *B*). We hypothesized that the higher concentrations of DTDP led to increased liberation of intracellular Zn^{2+}, which, in turn could somehow antagonize the activity of the phosphatase. As such, we first confirmed that, indeed, neurons treated with 60 μM DTDP exhibited a significant increase in TPEN-sensitive Zn^{2+} fluorescence (ΔF_{TPEN}) when compared to neurons treated with 30 μM DTDP (Fig. 6*C*). Secondly, to test whether Cyt-PTPε enzymatic activity is inhibited by Zn^{2+}, we performed an *in vitro* phosphatase assay (Promega) using Cyt-PTPε immunopurified from CHO cells expressing the phosphatase. As shown in Fig. 7, we observed a 50% inhibition in Cyt-PTPε activity in cells previously treated with 100 μM Zn^{2+} and 1 μM of the Zn^{2+}-selective ionophore pyrithione (ZnPyr). It is noteworthy that this stimulus was utilized for these experiments instead of DTDP, as we found it difficult to recover sufficient amounts of protein from oxidant-treated cells to perform the assay. Importantly, the inhibitory actions of Zn^{2+} on Cyt-PTPε were prevented in enzyme preparations that had been isolated from cells treated with ZnPyr in the presence of 10 μM TPEN (Fig. 7). Moreover, a consistent increase in phosphatase activity was observed in Cyt-PTPε isolated from cells treated with TPEN alone (Fig. 7). This suggests that basal levels of endogenous Zn^{2+} can inhibit Cyt-PTPε enzymatic activity, which could partly account for the large current densities observed in Kv2.1(S800D)-expressing CHO cells. More importantly, these results indicate that Zn^{2+}-mediated inhibition of Cyt-PTPε may operate in parallel to Zn^{2+}-induced p38 activation following DTDP treatment to trigger the apoptotic surge of Kv2.1-mediated K^+ currents.

Over-expression of Cyt-PTPε attenuates neuronal cell death

In the final set of studies, we investigated whether Cyt-PTPε over-expression would be sufficient to protect cortical neurons from injury. We chose to use exposure of neurons to activated microglia, as we have recently observed that this pathophysiologically relevant injurious

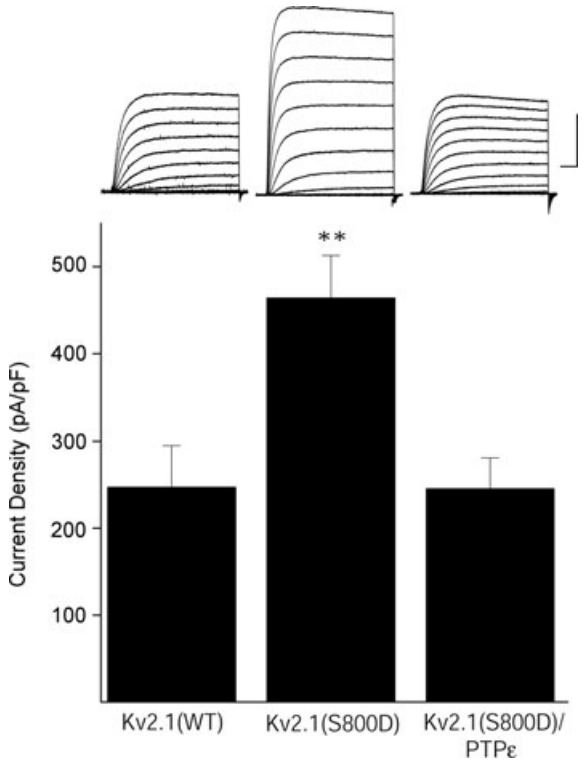

Figure 5. Cyt-PTPε inhibits elevated basal K^+ currents mediated by Kv2.1(S800D) mutant channels
Top, representative whole-cell K^+ currents from wild-type Kv2.1-, Kv2.1(S800D)- and Cyt-PTPε-expressing CHO cells. Currents were obtained 24 h post-transfection, 3 h post-oxidative injury, and evoked by sequential 10 mV voltage steps to +80 mV from a holding potential of −80 mV. Calibration: 5 nA, 25 ms. Bottom, mean ± S.E.M. current densities from wt Kv2.1- ($n = 14$), Kv2.1(S800D)- ($n = 11$), or Kv2.1(S800D) and Cyt-PTPε-expressing CHO cells ($n = 15$) (**$P < 0.01$; ANOVA/Dunnett).

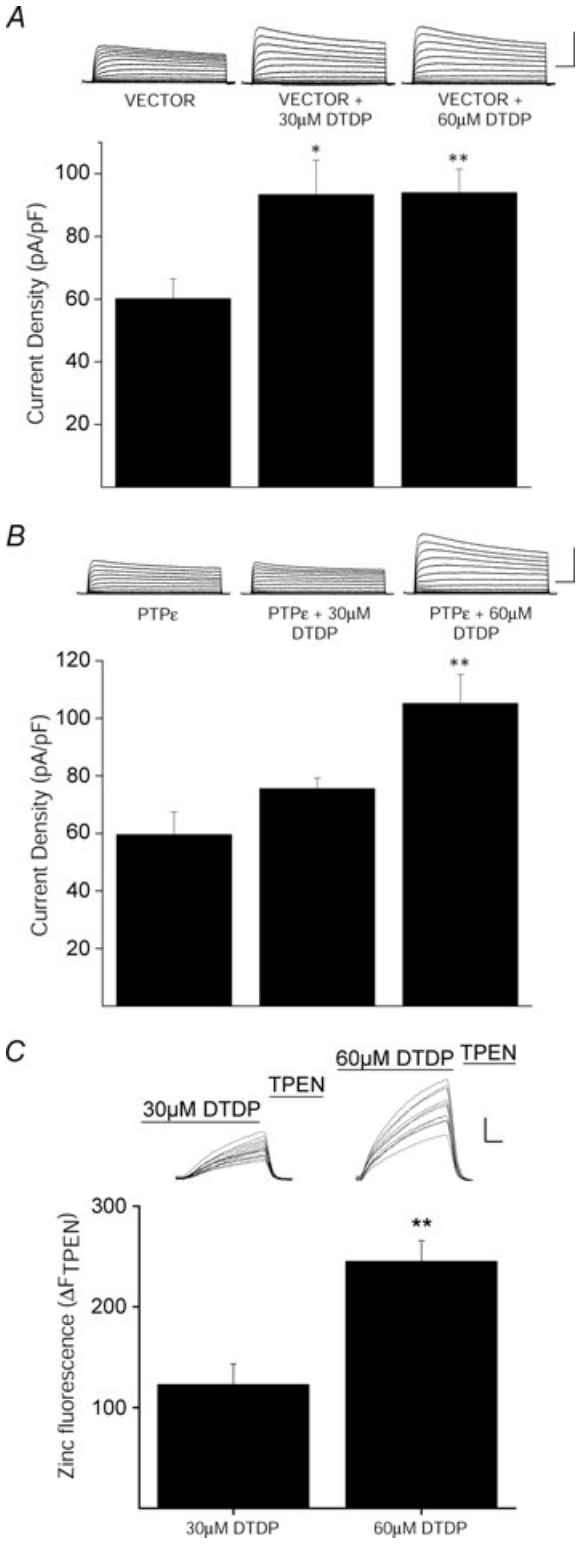

Figure 6. Cyt-PTPε inhibition of apoptotic K^+ current enhancement is Zn^{2+} dependent
A, K^+ currents are enhanced in vector-expressing cortical neurons following oxidative injury. Top, representative whole-cell K^+ currents from cortical neurons co-transfected with empty pRBG4-vector eGFP recorded following vehicle and DTDP treatment conditions (30 μM or 60 μM for 10 min). Calibration: 5 nA, 25 ms. Bottom, mean ± S.E.M. current densities from empty pRBG4-vector- and eGFP-expressing cortical neurons recorded under control ($n = 12$) and DTDP (30 μM, $n = 17$; 60 μM, $n = 10$) treatment conditions (*$P < 0.05$, **$P < 0.01$; ANOVA/Tukey). Current density was calculated as the steady-state K^+ current evoked by a single voltage step to +10 mV from a holding potential of −80 mV normalized to cell capacitance. *B*, inhibition of apoptotic K^+ current enhancement by Cyt-PTPε is Zn^{2+} dependent in cortical neurons. Top, representative whole-cell K^+ currents from Cyt-PTPε- and eGFP-expressing cortical neurons recorded under control and DTDP treatment conditions. Calibration: 5 nA, 25 ms. Bottom, mean ± S.E.M. current densities from Cyt-PTPε- and eGFP-expressing cortical neurons recorded under control ($n = 12$) and DTDP (30 μM, $n = 6$; 60 μM, $n = 10$) treatment conditions (*$P < 0.01$; ANOVA/Tukey). *C*, increasing DTDP concentration increases intracellular-free Zn^{2+}. Neurons loaded with the Zn^{2+}-specific indicator, FluoZin-3, were exposed to 30 μM or 60 μM DTDP. The DTDP-induced Zn^{2+} signal was quenched with superfusion of TPEN (20 μM). Inset, representative fluorescence traces of several neurons in a single coverslip. Each trace reflects the level of intracellular Zn^{2+} in a single neuron. Calibration: 100 arbitrary fluorescence units, 100 s. Plot shows TPEN-sensitive Zn^{2+} fluorescence, expressed as ΔF_{TPEN}, which was determined by subtracting the fluorescence signal after TPEN superfusion from the maximal DTDP-induced signal. Data represent the mean (± S.E.M.) ΔF_{TPEN} measurements from 5–6 coverslips, each containing 10–25 neurons (**$P < 0.01$; two-tailed *t* test).

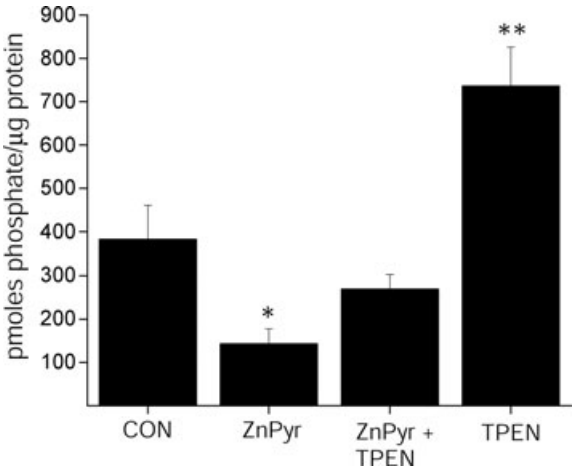

Figure 7. Cyt-PTPε catalytic activity is inhibited by Zn^{2+}
Cyt-PTPε was purified by immunoprecipitation from whole CHO cell lysates treated with either vehicle, Zn^{2+} (100 μM) + pyrithione (1 μM), Zn^{2+} + pyrithione + TPEN (10 μM), or TPEN, and added to a phosphatase assay containing 2 synthetic phosphotyrosine peptide substrates. Activity was normalized to Cyt-PTPε recovered following immunoprecipitation and elution and is expressed as pmoles phosphate generated per μg protein (mean ± S.E.M., $n = 6$, significantly different from control, *$P < 0.05$, **$P < 0.01$, ANOVA/Dunnett).

stimulus induced neuronal death that was characterized by elevated intracellular Zn^{2+} levels and a pronounced apoptotic K^+ current surge (Knoch *et al.* 2008). Indeed, vector-transfected neurons exhibited the expected robust, characteristic K^+ current surge following exposure to activated microglia (Fig. 8*A*). In contrast, K^+ currents

were not enhanced in neurons transfected with Cyt-PTPε (Fig. 8*B*). Importantly, over-expression of the phosphatase was sufficient to significantly reduce microglial-mediated toxicity in neurons (Fig. 8*C*). Cyt-PTPε-expressing neurons displayed an approximate 2-fold increase in viability compared to vector-expressing neurons exposed to activated microglia (Fig. 8*C*), resembling the neuroprotection observed in previous studies using Kv2.1 dominant negative isoforms (Pal *et al.* 2003; Knoch *et al.* 2008). Taken together, these data suggest that Cyt-PTPε over-expression confers neuroprotection by its inhibitory influence on the K^+ current surge following an apoptotic insult.

Discussion

Several phosphorylation targets in Kv2.1 have been shown to influence the voltage-dependent gating properties of this potassium channel (Park *et al.* 2006). In those instances, the Ca^{2+}-activated phosphatase calcineurin mediates the dephosphorylation of numerous intracellular sites that cooperate in the graded regulation of the channel (Park *et al.* 2006). However, the phosphorylation sites described in our studies, Y124 and S800, are not calcineurin targets (Park *et al.* 2006), nor do they participate in Kv2.1 modulation during non-apoptotic conditions. Our present results show that a functional, intact Y124 is necessary, regardless of the phosphorylation

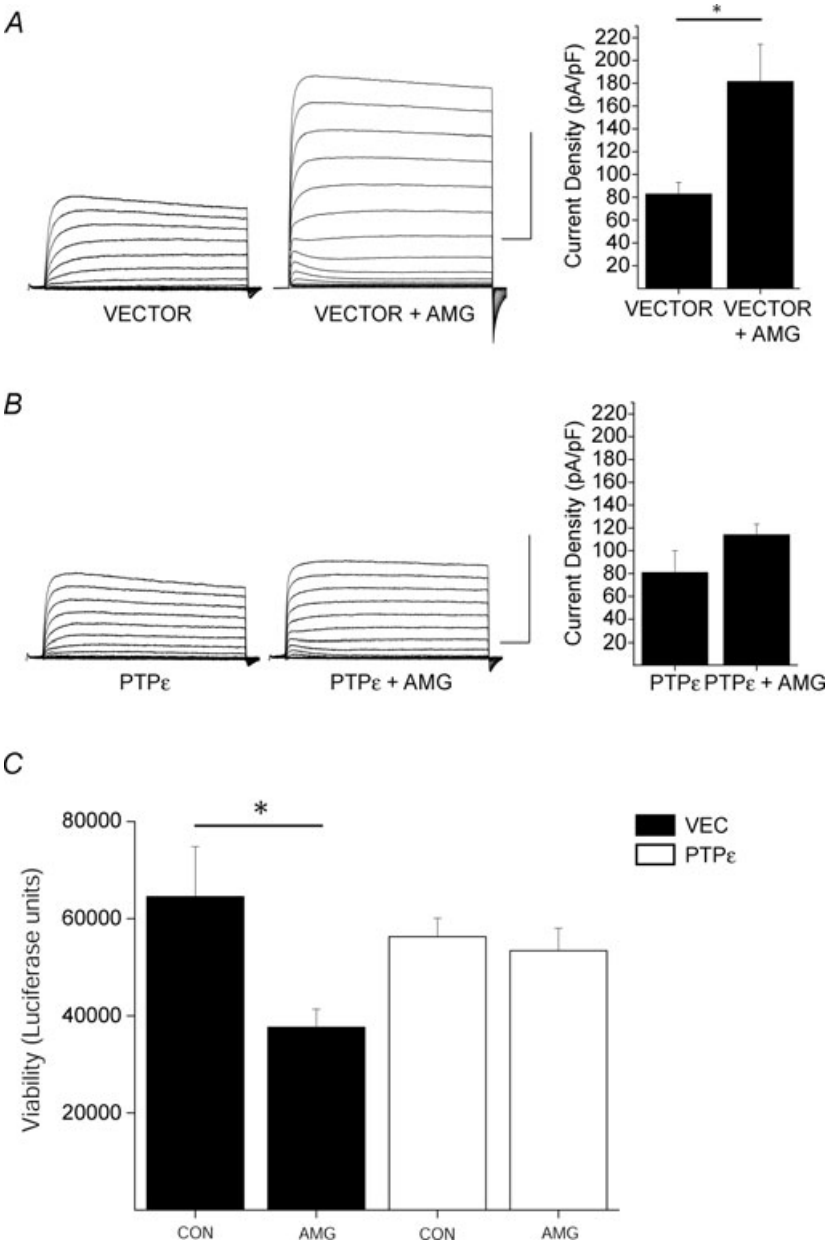

Figure 8. Over-expression of Cyt-PTPε blocks Kv2.1-mediated neuronal cell death
A, K^+ currents are enhanced in vector-expressing cortical neurons following exposure to activated microglia. Left, representative whole-cell K^+ currents from cortical neurons co-transfected with empty pcDNA-vector and eGFP and recorded following vehicle and activated microglial (AMG) treatment conditions. Calibration: 10 nA, 25 ms. Right, mean ± S.E.M. current densities from empty pcDNA-vector- and eGFP-expressing cortical neurons recorded under control ($n = 6$) and DTDP ($n = 7$) treatment conditions (*$P < 0.01$; 2-tailed *t* test). Current density was calculated as the steady-state K^+ current evoked by a single voltage step to +10 mV from a holding potential of −80 mV normalized to cell capacitance. *B*, over-expression of Cyt-PTPε blocks apoptotic K^+ current densities in cortical neurons. Left, representative whole-cell K^+ currents from Cyt-PTPε- and eGFP-expressing cortical neurons recorded under control and microglial treatment conditions. Calibration: 10 nA, 25 ms. Right, mean ± S.E.M. current densities from Cyt-PTPε- and eGFP-expressing cortical neurons recorded under control ($n = 6$) and microglial ($n = 7$) treatment conditions. *C*, Cyt-PTPε over-expression blocks neuronal cell death following exposure to activated microglia. Viability was assayed 24 h post-treatment by luciferase activity and expressed as luciferase units. Values represent the mean ± S.E.M. viability from each condition performed in quadruplicate and are representative of 5 separate, independent experiments. (*$P < 0.05$, ANOVA/Tukey).

status of S800 (Redman *et al.* 2007), for Kv2.1-mediated current enhancement to proceed during apoptosis. Therefore, Y124 and S800 act as coordinated molecular checkpoints mediating the apoptotic K^+ current surge and are critical determinants for neuronal viability. Remarkably, the cation ultimately controlling Kv2.1 channel modulation at Y124 and S800 is Zn^{2+}, not Ca^{2+}.

Elson and colleagues identified Y124 as a novel substrate for direct phosphorylation and dephosphorylation reactions by Src kinase and Cyt-PTPε, respectively (Tiran *et al.* 2003). However, the role of Y124 on apoptosis had not been previously evaluated. Our results indicate that Y124 is, in fact, a critical residue in the support of the obligatory K^+ current enhancement in dying cortical neurons. Nonetheless, this N-terminal residue must work in concert with S800, as a serine-to-alanine point mutation at this C-terminal location is sufficient to abolish the current surge and prevent cell death (Redman *et al.* 2007). The molecular mechanism leading to Kv2.1 plasma membrane insertion (Pal *et al.* 2006) following channel modulation remains to be addressed.

Although Src can be activated by intracellular Zn^{2+} (Wu *et al.* 2002), Zn^{2+}-activated Src cannot account for enhanced K^+ currents observed under all conditions, since CHO cells expressing Kv2.1(S800D) mutant channels still exhibit elevated currents without DTDP treatment (Figs 1*C* and 5). This suggests that basal levels of Src activity are present in these cells, which can also account for the decreased current densities observed in Kv2.1(S800D)-expressing cells co-transfected with Cyt-PTPε (Fig. 7). However, as pharmacological inhibition of Src is sufficient to block injury-dependent K^+ current surge in neurons (Fig. 2), some level of Zn^{2+}-mediated Src activity is likely to be an important component in the apoptotic surge of K^+ currents in the brain.

The present study has also established that the overall balance between Y124 phosphorylation and dephosphorylation is strongly modulated by Zn^{2+}, as our data show that Zn^{2+} can inhibit Cyt-PTPε. Indeed, other types of protein phosphatases have been previously shown to be inhibited by this metal (Brautigan *et al.* 1981; Gil-Henn *et al.* 2001; Meng *et al.* 2002; Haase & Maret, 2003, 2005; Toledano-Katchalski *et al.* 2003; Tal *et al.* 2006), including the MAPK phosphatase PP2A (Ho *et al.* 2008). The fact that Zn^{2+} can directly act on the highly conserved active site of protein tyrosine phosphatases at nanomolar concentrations (Haase & Maret, 2003) is highly suggestive that Zn^{2+} may not only inhibit Cyt-PTPε directly, but may also exert powerful inhibitory effects on many PTPs, including others enzymes that may target Y124. We recognize, however, that Zn^{2+} may inhibit Cyt-PTPε by other mechanisms. Indeed, Cyt-PTPε forms inactive monomeric and dimeric species under basal conditions, which tend to stabilize during oxidative stress (Toledano-Katchalski *et al.* 2003). Whether Zn^{2+} participates in this process has yet to be determined.

The convergence of multiple enzymatic signalling pathways upon ion channels has been previously observed, albeit in non-injurious conditions. Moult *et al.* (2008) showed that p38 and an unspecified protein tyrosine phosphatase co-modify mGLuR2 subunits of AMPARs to mediate receptor internalization and long-term depression in the CA1 region of the rat hippocampus (Moult *et al.* 2008). Our work suggests a disruption in tyrosine phosphatase activity together with coordinated action of Src kinase and p38 MAPK activity by Zn^{2+} during apoptosis (Fig. 9). Thus, the liberation of intracellular

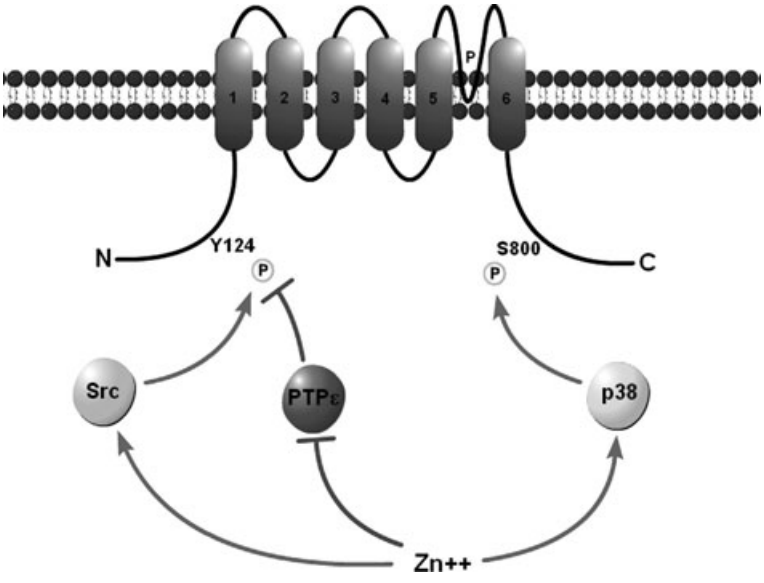

Figure 9. Schematic of Kv2.1 illustrating the proposed effect of intracellular Zn^{2+} on the checkpoint-modifying enzymes src, Cyt-PTPε and p38
The apoptotic K^+ current surge observed in neuronal apoptosis is mediated by surface delivery of Kv2.1-encoded ion channels when intracellular residues Y124 and S800 are phosphorylated. This state is achieved following intracellular Zn^{2+} liberation, which increases kinase activity while inhibiting phosphatase activity.

Zn^{2+} serves as a common upstream signal favouring the phosphorylation of Kv2.1 residues Y124 and S800. As such, we define here an essential regulatory event in the apoptotic program, where distinct Zn^{2+}-dependent signalling cascades converge upon Kv2.1 to mediate the apoptotic K^+ current surge during neuronal cell death.

References

Aizenman CD, Akerman CJ, Jensen KR & Cline HT (2003). Visually driven regulation of intrinsic neuronal excitability improves stimulus detection *in vivo*. *Neuron* **39**, 831–842.

Aizenman E, Sinor JD, Brimecombe JC & Herin GA (2000*a*). Alterations of N-methyl-D-aspartate receptor properties after chemical ischemia. *J Pharmacol Exp Ther* **295**, 572–577.

Aizenman E, Stout AK, Hartnett KA, Dineley KE, McLaughlin B & Reynolds IJ (2000*b*). Induction of neuronal apoptosis by thiol oxidation: putative role of intracellular zinc release. *J Neurochem* **75**, 1878–1888.

Aras MA & Aizenman E (2005). Obligatory role of ASK1 in the apoptotic surge of K^+ currents. *Neurosci Lett* **387**, 136–140.

Aras MA, Hartnett KA & Aizenman E (2008). Assessment of cell viability in primary neuronal cultures. *Curr Protoc Neurosci* Chapter 7, Unit 7.18.

Boeckman FA & Aizenman E (1996). Pharmacological properties of acquired excitotoxicity in Chinese hamster ovary cells transfected with N-methyl-D-aspartate receptor subunits. *J Pharmacol Exp Ther* **279**, 515–523.

Bossy-Wetzel E, Talantova MV, Lee WD, Scholzke MN, Harrop A, Mathews E, Gotz T, Han J, Ellisman MH, Perkins GA & Lipton SA (2004). Crosstalk between nitric oxide and zinc pathways to neuronal cell death involving mitochondrial dysfunction and p38-activated K^+ channels. *Neuron* **41**, 351–365.

Brautigan DL, Bornstein P & Gallis B (1981). Phosphotyrosyl-protein phosphatase. Specific inhibition by Zn. *J Biol Chem* **256**, 6519–6522.

Cheepsunthorn P, Radov L, Menzies S, Reid J & Connor JR (2001). Characterization of a novel brain-derived microglial cell line isolated from neonatal rat brain. *Glia* **35**, 53–62.

Daum G, Solca F, Diltz CD, Zhao Z, Cool DE & Fischer EH (1993). A general peptide substrate for protein tyrosine phosphatases. *Anal Biochem* **211**, 50–54.

Drummond GB (2009). Reporting ethical matters in *The Journal of Physiology*: standards and advice. *J Physiol* **587**, 713–719.

Flint AJ, Tiganis T, Barford D & Tonks NK (1997). Development of 'substrate-trapping' mutants to identify physiological substrates of protein tyrosine phosphatases. *Proc Natl Acad Sci U S A* **94**, 1680–1685.

Gil-Henn H, Volohonsky G & Elson A (2001). Regulation of protein-tyrosine phosphatases α and ε by calpain-mediated proteolytic cleavage. *J Biol Chem* **276**, 31772–31779.

Haase H & Maret W (2003). Intracellular zinc fluctuations modulate protein tyrosine phosphatase activity in insulin/insulin-like growth factor-1 signalling. *Exp Cell Res* **291**, 289–298.

Haase H & Maret W (2005). Protein tyrosine phosphatases as targets of the combined insulinomimetic effects of zinc and oxidants. *Biometals* **18**, 333–338.

Ho Y, Samarasinghe R, Knoch ME, Lewis M, Aizenman E & Defranco DB (2008). Selective inhibition of MAPK phosphatases by zinc accounts for ERK1/2-dependent oxidative neuronal cell death. *Mol Pharmacol* **74**, 1141–1151.

Huang YZ, Pan E, Xiong ZQ & McNamara JO (2008). Zinc-mediated transactivation of TrkB potentiates the hippocampal mossy fiber-CA3 pyramid synapse. *Neuron* **57**, 546–558.

Hughes FM Jr & Cidlowski JA (1999). Potassium is a critical regulator of apoptotic enzymes *in vitro* and *in vivo*. *Adv Enzyme Regul* **39**, 157–171.

Knoch ME, Hartnett KA, Hara H, Kandler K & Aizenman E (2008). Microglia induce neurotoxicity via intraneuronal Zn^{2+} release and a K^+ current surge. *Glia* **56**, 89–96.

Leung YM, Kang Y, Gao X, Xia F, Xie H, Sheu L, Tsuk S, Lotan I, Tsushima RG & Gaisano HY (2003). Syntaxin 1A binds to the cytoplasmic C terminus of Kv2.1 to regulate channel gating and trafficking. *J Biol Chem* **278**, 17532–17538.

Lvov A, Chikvashvili D, Michaelevski I & Lotan I (2008). VAMP2 interacts directly with the N terminus of Kv2.1 to enhance channel inactivation. *Pflugers Arch* **456**, 1121–1136.

MacDonald PE, Wang G, Tsuk S, Dodo C, Kang Y, Tang L, Wheeler MB, Cattral MS, Lakey JR, Salapatek AM, Lotan I & Gaisano HY (2002). Synaptosome-associated protein of 25 kilodaltons modulates Kv2.1 voltage-dependent K^+ channels in neuroendocrine islet beta-cells through an interaction with the channel N terminus. *Mol Endocrinol* **16**, 2452–2461.

McLaughlin B, Pal S, Tran MP, Parsons AA, Barone FC, Erhardt JA & Aizenman E (2001). p38 activation is required upstream of potassium current enhancement and caspase cleavage in thiol oxidant-induced neuronal apoptosis. *J Neurosci* **21**, 3303–3311.

Malin SA & Nerbonne JM (2002). Delayed rectifier K^+ currents, I_K, are encoded by Kv2 α-subunits and regulate tonic firing in mammalian sympathetic neurons. *J Neurosci* **22**, 10094–10105.

Meng TC, Fukada T & Tonks NK (2002). Reversible oxidation and inactivation of protein tyrosine phosphatases *in vivo*. *Mol Cell* **9**, 387–399.

Mohapatra DP, Siino DF & Trimmer JS (2008). Interdomain cytoplasmic interactions govern the intracellular trafficking, gating, and modulation of the Kv2.1 channel. *J Neurosci* **28**, 4982–4994.

Moult PR, Correa SA, Collingridge GL, Fitzjohn SM & Bashir ZI (2008). Co-activation of p38 mitogen-activated protein kinase and protein tyrosine phosphatase underlies metabotropic glutamate receptor-dependent long-term depression. *J Physiol* **586**, 2499–2510.

Murakoshi H & Trimmer JS (1999). Identification of the Kv2.1 K^+ channel as a major component of the delayed rectifier K^+ current in rat hippocampal neurons. *J Neurosci* **19**, 1728–1735.

Ohki EC, Tilkins ML, Ciccarone VC & Price PJ (2001). Improving the transfection efficiency of post-mitotic neurons. *J Neurosci Methods* **112**, 95–99.

Pal S, Hartnett KA, Nerbonne JM, Levitan ES & Aizenman E (2003). Mediation of neuronal apoptosis by Kv2.1-encoded potassium channels. *J Neurosci* **23**, 4798–4802.

Pal SK, Takimoto K, Aizenman E & Levitan ES (2006). Apoptotic surface delivery of K^+ channels. *Cell Death Differ* **13**, 661–667.

Park KS, Mohapatra DP, Misonou H & Trimmer JS (2006). Graded regulation of the Kv2.1 potassium channel by variable phosphorylation. *Science* **313**, 976–979.

Peretz A, Gil-Henn H, Sobko A, Shinder V, Attali B & Elson A (2000). Hypomyelination and increased activity of voltage-gated K^+ channels in mice lacking protein tyrosine phosphatase ε. *EMBO J* **19**, 4036–4045.

Pratt KG & Aizenman CD (2007). Homeostatic regulation of intrinsic excitability and synaptic transmission in a developing visual circuit. *J Neurosci* **27**, 8268–8277.

Redman PT, He K, Hartnett KA, Jefferson BS, Hu L, Rosenberg PA, Levitan ES & Aizenman E (2007). Apoptotic surge of potassium currents is mediated by p38 phosphorylation of Kv2.1. *Proc Natl Acad Sci U S A* **104**, 3568–3573.

Santos S & Aizenman E (2002). Functional expression of muscle-type nicotinic acetylcholine receptors in rat forebrain neurons *in vitro*. *Methods Find Exp Clin Pharmacol* **24**, 63–66.

Sensi SL & Jeng JM (2004). Rethinking the excitotoxic ionic milieu: the emerging role of Zn^{2+} in ischemic neuronal injury. *Curr Mol Med* **4**, 87–111.

Tal TL, Graves LM, Silbajoris R, Bromberg PA, Wu W & Samet JM (2006). Inhibition of protein tyrosine phosphatase activity mediates epidermal growth factor receptor signalling in human airway epithelial cells exposed to Zn^{2+}. *Toxicol Appl Pharmacol* **214**, 16–23.

Tiran Z, Peretz A, Attali B & Elson A (2003). Phosphorylation-dependent regulation of Kv2.1 channel activity at tyrosine 124 by Src and by protein-tyrosine phosphatase ε. *J Biol Chem* **278**, 17509–17514.

Tiran Z, Peretz A, Sines T, Shinder V, Sap J, Attali B & Elson A (2006). Tyrosine phosphatases ε and α perform specific and overlapping functions in regulation of voltage-gated potassium channels in Schwann cells. *Mol Biol Cell* **17**, 4330–4342.

Toledano-Katchalski H, Tiran Z, Sines T, Shani G, Granot-Attas S, den Hertog J & Elson A (2003). Dimerization *in vivo* and inhibition of the nonreceptor form of protein tyrosine phosphatase ε. *Mol Cell Biol* **23**, 5460–5471.

Tsuk S, Michaelevski I, Bentley GN, Joho RH, Chikvashvili D & Lotan I (2005). Kv2.1 channel activation and inactivation is influenced by physical interactions of both syntaxin 1A and the syntaxin 1A/soluble N-ethylmaleimide-sensitive factor-25 (t-SNARE) complex with the C terminus of the channel. *Mol Pharmacol* **67**, 480–488.

Weiss JH, Sensi SL & Koh JY (2000). Zn^{2+}: a novel ionic mediator of neural injury in brain disease. *Trends Pharmacol Sci* **21**, 395–401.

Wu W, Graves LM, Gill GN, Parsons SJ & Samet JM (2002). Src-dependent phosphorylation of the epidermal growth factor receptor on tyrosine 845 is required for zinc-induced Ras activation. *J Biol Chem* **277**, 24252–24257.

Yu SP (2003). Na^+,K^+-ATPase: the new face of an old player in pathogenesis and apoptotic/hybrid cell death. *Biochem Pharmacol* **66**, 1601–1609.

Yu SP & Kerchner GA (1998). Endogenous voltage-gated potassium channels in human embryonic kidney (HEK293) cells. *J Neurosci Res* **52**, 612–617.

Yu SP, Yeh CH, Sensi SL, Gwag BJ, Canzoniero LM, Farhangrazi ZS, Ying HS, Tian M, Dugan LL & Choi DW (1997). Mediation of neuronal apoptosis by enhancement of outward potassium current. *Science* **278**, 114–117.

Zhang Y, Wang H, Li J, Jimenez DA, Levitan ES, Aizenman E & Rosenberg PA (2004). Peroxynitrite-induced neuronal apoptosis is mediated by intracellular zinc release and 12-lipoxygenase activation. *J Neurosci* **24**, 10616–10627.

Zhang ZY, Thieme-Sefler AM, Maclean D, McNamara DJ, Dobrusin EM, Sawyer TK & Dixon JE (1993). Substrate specificity of the protein tyrosine phosphatases. *Proc Natl Acad Sci U S A* **90**, 4446–4450.

Author contributions

P.T.R., K.A.H., M.A.A., E.S.L. and E.A. designed research. P.T.R., K.A.H. and M.A.A. performed research. P.T.R., K.A.H., M.A.A., E.S.L. and E.A. analysed data. P.T.R., K.A.H., M.A.A., E.S.L. and E.A. drafted and approved the paper. Experiments were performed in the laboratory of E.A.

Acknowledgements

We thank J. Connor, Pennsylvania State University for the microglial cell line, and A. Elson and J. Trimmer for the gifts of plasmids. This work was supported by NIH grants NS043277 (E.A.) and HL080632 (E.S.L.) and American Heart Association grant 0615388U (P.T.R.).